Biotechnology Reports 37 (2023) e00782

Contents lists available at ScienceDirect

Biotechnology Reports

journal homepage: www.elsevier.com/locate/btre

Research Article

Development and scale-up of rVSV-SARS-CoV-2 vaccine process using single use bioreactor

Christopher Ton [a,*], Victoria Stabile [a], Elizabeth Carey [a], Adam Maraikar [b], Travis Whitmer [c], Samantha Marrone [a], Nelson Lee Afanador [d], Igor Zabrodin [a], Greeshma Manomohan [e], Melissa Whiteman [f], Carl Hofmann [f]

[a] Vaccine Process Development, Merck & Co., Inc., West Point, Pennsylvania, 19486, United States
[b] Bioprocess Clinical Manufacturing & Technology, Merck & Co., Inc., West Point, Pennsylvania, 19486, United States
[c] Bioprocess Drug Substance Commercialization, Merck & Co., Inc., West Point, Pennsylvania, 19486, United States
[d] Biostatistics and Research Decision Sciences, Merck & Co., Inc., West Point, Pennsylvania, 19486, United States
[e] Currently at GlaxoSmithKline plc, King of Prussia, Pennsylvania, 19406, United States
[f] Analytical Research & Development, Merck & Co., Inc., West Point, Pennsylvania 19486, United States

ARTICLE INFO

Keywords:
VSVΔG-SARS-CoV-2
Closed process
Vero cells
Serum-free
Microcarriers
Single use bioreactor

ABSTRACT

The outbreak of the novel severe acute respiratory syndrome coronavirus 2 (SARS-CoV-2) that causes the Coronavirus Disease 2019 (COVID-19) has spread through the globe at an alarming speed. The disease has become a global pandemic affecting millions of people and created public health crises worldwide. Among many efforts to urgently develop a vaccine against this disease, we developed an industrial-scale closed, single use manufacturing process for V590, a vaccine candidate for SARS-CoV-2. V590 is a recombinant vesicular stomatitis virus (rVSV) genetically engineered to express SARS-CoV-2 glycoprotein. In this work, we describe the development and optimization of serum-free microcarrier production of V590 in Vero cells in a closed system. To achieve the maximum virus productivity, we optimized pH and temperature during virus production in 3 liters (L) bioreactors. Virus productivity was improved (by ~1 log) by using pH 7.0 and temperature at 34.0 °C. The optimal production condition was successfully scaled up to a 2000 L Single Use Bioreactor (SUB), producing a maximum virus titer of ~1.0e+7 plaque forming units (PFU)/mL. Further process intensification and simplification, including growing Vero cells at 2 gs per liter (g/L) of Cytodex-1 Gamma microcarriers and eliminating the media exchange (MX) step prior to infection helped to increase virus productivity by ~2-fold.

1. Introduction

COVID-19 is caused by the highly infectious SARS-CoV-2 virus. Coronaviruses are members of the subfamily *Coronavirinae* composed of four genera -*Alphacoronavirus, Betacoronavirus, Gammacoronavirus,* and *Deltacoronavirus,* in the family *Coronaviridae*, under the order *Nidovirales* [1,2]. SARS-CoV-2 was identified in Wuhan China in December 2019 [3]. On March 11, 2020, the World Health Organization (WHO) declared the global COVID-19 outbreak as a pandemic [4]. At the time of this authorship, there have been 511,479,320 confirmed cases of COVID-19, including 6238,832 deaths (https://covid19.who.int/). Among the several vaccines under development against COVID-19 is a rVSV that expresses another virus spike glycoprotein in place of the native VSV glycoprotein. The rVSV genetically engineered to express the glycoprotein of a Zaire Ebola virus was successfully used to develop ERVEBO®, the first licensed vaccine for the prevention of Ebola virus disease [5]. In collaboration with the International AIDS Vaccine Initiative (IAVI), we developed V590, a vaccine candidate for SARS-CoV-2. V590 is a recombinant vesicular stomatitis virus genetically engineered to express a SARS-CoV-2 glycoprotein.

The Vero cell line was the first continuous cell line (CCL) to be approved by the WHO for the manufacturing of viral vaccines for human use [6–8]. There has been over 30 years of experience with using Vero cells as substrates for human vaccines, with hundreds of million doses manufactured and distributed worldwide [9]. For adherent cell culture, there are several static cell culture systems that are available for vaccine production such as roller bottles and cell factories. However, large-scale production with these systems requires scaling out as opposed to scaling

* Corresponding author.
E-mail address: christopher.ton@merck.com (C. Ton).

https://doi.org/10.1016/j.btre.2023.e00782
Received 7 September 2022; Received in revised form 12 January 2023; Accepted 13 January 2023
Available online 16 January 2023
2215-017X/© 2023 Published by Elsevier B.V. This is an open access article under the CC BY-NC-ND license (http://creativecommons.org/licenses/by-nc-nd/4.0/).

up. Scaling-out could require large footprints for production facilities and increase manual processing which could greatly limit large-scale production of a viral vaccine. Other alternative systems to roller bottles and cell factories are fixed-bed or packed-bed systems such as the iCELLis® bioreactor (Pall) [10–12], Fibra-Cel® disks (Eppendorf) [13], and the scale-X™ bioreactor (Univercells) [14,15]. These systems typically rely on highly porous polyester microfiber carriers or disks, providing large growth surface matrices which can protect adherent cells against mechanical shear stress [16]. However, it is difficult to harvest cells from the matrices, making packed-bed bioreactors suboptimal for cell expansion purposes [17].

Although Vero cells have been adapted to grow in serum-free suspension cultures [18,19] and have been used for virus production, more research still needs to be done to improve the Vero suspension system [15]. Suspension Vero cells have low cell growth rates, with doubling time of more than 40 h. In addition, application of suspension Vero cells is also limited due to their dependence on in-house media [18,19]. Kiesslich et al. recently demonstrated the production of several vaccine candidates in suspension Vero cells with commercial medium MDXK (Xell AG, Germany). However, long doubling time of around 65 h and formation of cell aggregates still raise concerns [20].

For large-scale production of viral vaccines, the use of Vero cells cultured on microcarriers has been widely adopted [21–23] and process scale-up has been successfully demonstrated up to a 6000 L scale [21,6]. Conventional stainless-steel stirred tank bioreactors require high initial investment capital cost, long turn-around time between batches, and cleaning as well as steam sanitization validation. With the potential need for large numbers of vaccine doses to combat the COVID-19 pandemic quickly, it was crucial to develop an industrial-scale vaccine production process that can be implemented rapidly. Single Use Bioreactor offers an attractive option, as a SUB mimics the scalability and operating parameters of conventional stirred-tank bioreactors and has the advantage of being completely disposable [24]. In addition, production facilities utilizing disposables can be commissioned quickly during the pandemic, as the complexity involved in planning, installation, and validation of production facilities is reduced greatly [16].

In this study, we describe the development of a scalable, Good Manufacturing Practice (GMP) compliant, closed and fully disposable microcarrier-based bioreactor production process for an rVSV-SARS-CoV-2 vaccine candidate. The production process can be scaled up to a 2000 L SUB and generate 1.0e+7 PFU/mL of harvested virus.

2. Materials and methods

2.1. Cell line and static cell growth

The Vero cell line ATCC CCL-81.2 was obtained from the ATCC. Vero cells were maintained in static culture using OptiPRO™ Serum Free medium (Thermo Fisher Scientific) supplemented with 4 mM L-glutamine (Thermo Fisher Scientific) at 37 °C and 5% CO_2 in a humidified incubator (Thermo Scientific). Cells were passaged seven times to create a working cell bank, which was used for all experiments described herein. For static cell growth, cells were passaged for 4 passages in Corning CellSTACK® using TrypLE™ Select (ThermoFisher Scientific) for cell detachment and Soybean Trypsin Inhibitor (STI; 1 g/L) for protease inactivation (Millipore Sigma). Cell concentration and viability were determined using the Vi-CELL™ XR cell counter (Beckman Coulter, USA). All static cell growth manipulations were performed in a closed system via sterile welds and pumps, except for the initial vials thaw operation.

2.2. Virus

Virus rescue and amplification of VSVΔG-SARS-CoV-2 has been previously described [25]. The working virus seed stock used in this study was generated in Vero cells grown on 1 g/L Cytodex-1 Gamma microcarriers (Cytiva) in a 50 L SUB. Briefly, the master virus seed was used to infect Vero cells at a multiplicity of infection (MOI) of 0.001 plaque forming units per viable cell (PFU/vc). At 2 days post-infection (DPI), virus suspension from infected culture was harvested through a Harvestainer™ Microcarrier Separation System (ThermoFisher Scientific) for microcarriers separation and purified by ultrafiltration and stored in 10 mM Tris, 150 mM sodium chloride, pH 7.5 buffer formulated with 2.5 g/L recombinant human serum albumin. The purified working virus seed stock was aliquoted in Cryovaults® (Meissner) and vials, frozen and stored at –70 °C. A new aliquot of the virus seed stock was thawed for each experiment to avoid freeze-thaw.

2.3. N-1 Cell growth

N-1 bioreactor cultures were performed in 50 L and 250 L SUBs (ThermoFisher Scientific).

Using the harvested cell suspension from static cell growth, the bioreactor was inoculated with a seeding cell density of 1.3e+4 cells/cm^2 on 2 g/L of Cytodex-1 Gamma microcarriers (Cytiva). The medium VP-SFM was supplemented with 6 mM L-glutamine (ThermoFisher Scientific) and 0.1% (w/v) Poloxamer-188 (BASF, Germany). VP-SFM was used in microcarrier culture to improve cells growth and virus production (data not shown). Once inoculated, the bioreactor was controlled at 37 °C, pH 7.3 via CO_2 or Na_2CO_3 addition and dissolved oxygen (DO) was maintained at $\geq$ 50% saturation for approximately 4 days. Three days post cell inoculation (3 DPCI), an ~80% medium exchange (MX) was performed. On 4 DPCI, cells were harvested in situ enzymatically using TrypLE™ Select (ThermoFisher Scientific). Upon completion of trypsinization, 1 g/L STI (Millipore Sigma) was added to the bioreactor. Cells were separated from microcarriers using the Harvestainer™ Microcarrier Separation System (ThermoFisher Scientific). Cell concentration and viability were determined using the Vi-CELL™ XR cell counter (Beckman Coulter, USA). Similar to the static cell growth, all process manipulations were performed in a closed system via sterile welds, aseptic connectors, and pumps.

2.4. Process optimization and simplification for rVSV-SARS-CoV-2 production in 3 L bioreactors

Process optimization was performed with Eppendorf BioFlo320 3 L glass bioreactors with pitched 3-blade impellers and a 3 L working volume. Cells from static cell growth were used to inoculate the 3 L bioreactors with 1 g/L Cytodex-1 Gamma microcarriers (Cytiva) at 1.3e+4 cells/cm^2. The medium VP-SFM was supplemented with 4 mM L-glutamine (ThermoFisher Scientific) and 0.1% (w/v) Poloxamer-188 (BASF, Germany) for shear protection. Bioreactors were controlled at 37 °C and agitated at 42 rpm (RPM) for the first 2 days of cell growth. To maintain microcarriers in suspension as the cells continued to grow, the agitation was increased to 47 RPM on 2 DPCI and again to 52 RPM on 5 DPCI. Cells were grown in the bioreactor for 5 days at 37 °C. DO was maintained at $\geq$ 50% saturation by oxygen sparge. The pH was maintained at 7.3 through CO_2 overlay or Na_2CO_3 addition. On 5 DPCI an 80% MX was performed for each bioreactor by settle-decant and fresh media for infection was added. After MX, temperature was controlled at the infection set point of 34 °C; pH set point was changed after virus addition to 7.0. For the optimization study, cells were infected at a MOI of 0.001 by fixed surface area (PFU/cm^2). During growth and infection, L-glutamine was supplemented to 4 mM if the concentration fell below 2 mM.

To improve process efficiency, the feasibility of not performing a MX step prior to infection was evaluated. The evaluation of no MX process was done with the same Eppendorf BioFlo320 3 L glass bioreactors as described above. Cells from N-1 bioreactor were used to inoculate six glass bioreactors with 1 g/L Cytodex 1 Gamma microcarriers and inoculated at 2.2e+4 cells/cm^2. On 5 DPCI, MX was only performed for control bioreactors ($n = 3$) and not the experimental no MX arm ($n = 3$).

All bioreactors were infected with a MOI of 0.001 by cell density (PFU/vc). For virus production, bioreactors were maintained at a temperature of 34 °C and a pH of 7.0.

2.5. Process intensification for rVSV-SARS-CoV-2 production in 2 L bioreactor

To intensify the process for rVSV-SARS-CoV-2 production, different microcarrier concentrations were evaluated for virus productivity in 2 L glass bioreactors. Process intensification studies utilized 2 L Univessel Glass bioreactors with BioStat® B-DCU II towers (Sartorius Stedim). Three different concentrations of microcarriers were evaluated at 1 g/L, 2 g/L, and 3 g/L. Vero cells were grown in a N-1 bioreactor with 2 g/L Cytodex 1 microcarriers as described above. On 4 DPCI, Cytodex 1 with cells attached were removed from the 250 L bioreactor and transferred to the 2 L bioreactors with $n = 2$ bioreactors for 2 g/L and 3 g/L Cytodex 1 and $n = 1$ for 1 g/L Cytodex 1.

To calculate the volume of Cytodex 1 suspension required from the N-1 to achieve the appropriate concentrations in 2 L bioreactors, the equation $(C_{N-1} \times V_{N-1}) = (C_{2LBR} \times V_{2LBR})$ was used; representing the concentration and volume of N-1 suspension required to achieve a target g/L Cytodex 1 concentration at a 1.6 L initial volume. The removed Cytodex 1 suspension from N-1 was allowed to settle, residual media was aspirated out, and the remaining volume was resuspended with fresh media to reach the required working volume in the bioreactor. This MX step was also performed for the 2 g/L Cytodex 1 condition despite matching the Cytodex 1 concentration of the N-1 to provide fresh VP-SFM that matched other conditions. The bioreactors equilibrated at 37 °C and a pH of 7.3 prior to virus infection. Bioreactors were infected with an MOI of 0.001 by cell density (PFU/vc) and then controlled at 34 °C and pH 7.0 for the virus production period.

2.6. Closed system transfer of Gamma-irradiated Cytodex 1 microcarriers for large-scale bioreactors

Cytodex 1 Gamma microcarriers were aliquoted and transferred via closed system to maintain sterility. To ensure that the appropriate amount of Cytodex 1 was aliquoted, microcarriers were first transferred from the stock container to a 2 L dispense container. The specially designed 2 L PETG bottle was sterile welded to the Cytodex 1 stock container, placed on a scale and microcarriers were transferred via gravity and assisted by the bioreactor air mass flow controller. After the aliquot was complete, the 2 L PETG bottle was welded onto the bioreactor, and the bioreactor air mass flow controller was used to transfer Cytodex 1 from the dispense container into the bioreactor, where they were hydrated by media during batching.

2.7. Large-scale production of rVSV-SARS-CoV-2

The N-stage production process of rVSV-SARS-CoV-2 was developed in a SUB (ThermoFisher Scientific). All bioreactor operations were conducted using single use consumables and within a closed system. The single use bioprocess container was designed with a 2:1 standard impeller and Aegis 5–14 film. Processes were developed at three scales: 50 L, 500 L, and the manufacturing scale at 2000 L. Cytodex-1 Gamma microcarriers were dry dispensed into the bioreactor prior to batching and hydrated in media to a concentration of 1 g/L. The medium VP-SFM was supplemented with 6 mM L-glutamine and 0.1% Poloxamer-188 (BASF, Germany). Immediately following the N-1 bioreactor harvest, cells were inoculated in the N-stage bioreactor with a seeding cell density of 2.2e+4 cells/cm^2.

During the growth phase, temperature was maintained at 37 °C and pH was controlled at 7.3, via CO_2 or Na_2CO_3 addition. DO was maintained at $\geq$ 50% saturation. Gas addition to the bioreactor via sparge was avoided to minimize disrupting the attachment of cells to microcarriers. Agitation rates were scaled up using power per unit volume calculations, so that there was a constant power per unit volume at all scales, from 2 to 2000 L. At the 50 L scale, agitation was 75 RPM at cell inoculation and increased to 85 RPM at 2 DPCI. These agitation rates corresponded to 35 and 43 RPM in the 500 L bioreactor and 30 and 35 RPM in the 2000 L bioreactor respectively. Bioreactors were checked visually each day to confirm that no settling had occurred as the microcarriers became heavier and more confluent with dividing cells.

On 5 DPCI, an 80% MX was performed via settling of the microcarriers, decant of spent media, and addition of fresh media. After MX, the bioreactor was temperature controlled to 34 °C before virus was added. The bioreactor was infected with rVSV-SARS-CoV-2 at an MOI of 0.001 PFU/vc. Upon virus addition, the pH set point was changed to 7.0, using carbon dioxide. DO was maintained at $\geq$ 50% saturation. The bioreactor was harvested on 2 DPI. A Harvestainer™ Microcarrier Separation System (ThermoFisher) was used to separate microcarriers from the harvested virus.

2.8. Process intensification and simplification for rVSV-SARS-CoV-2 production in 50 L bioreactor

Process intensification and simplification studies conducted at 2 and 3 L scale were demonstrated in 50 L bioreactors. An experiment was conducted to test the intensification strategy of increasing the Cytodex 1 concentration while maintaining a seeding cell density of 2.2e+4 cells/cm^2. The control bioreactor was run at baseline conditions of 1 g/L Cytodex 1 Gamma with a 5 DPCI MX prior to infection. The second bioreactor tested a 2-fold increase (2 g/L) of the Cytodex 1 Gamma concentration in the bioreactor. All process operating parameters were kept consistent between the two conditions except for agitation. For the 1 g/L condition, agitation schemes were as described above. For the 2 g/L culture, agitation at the start of the experiment followed the control condition of 75 RPM at cell inoculation, but then increased to 85 RPM at 1 DPCI, increased to 95 RPM at 4 DPCI, and finally set to 105 RPM at infection. Higher agitation rates for the 2 g/L condition were necessary to ensure adequate suspension of microcarriers.

Process simplification was also studied to determine if removal of MX operations affects cells growth and virus production. A 50 L bioreactor was setup up and ran at baseline conditions as described in the section above, however the MX step was eliminated. Eliminating MX steps is favorable as it would reduce manual operations and is cost effective due to the reduced media consumption.

2.9. Bioreactor sampling procedures

Bioreactors were sampled each day during growth and infection. Samples were analyzed for nutrients and metabolites with Nova Bioprofile Flex or Flex2 (Nova Biomedical, USA) and cell density with NucleoCounter NC-200 (Chemometec, Denmark). During growth and infection, metabolite analysis was performed offline from fresh samples taken from the bioreactors. During infection, additional samples were taken at various timepoints as dictated by experimental design, frozen with 10% sucrose, and analyzed for infectivity by Plaque or microplaque (μPlaque) assay. Note, for 3 L bioreactor studies only, at the time of experimentation, the 0.5 DPI naming convention was used to indicate the second (afternoon) set of samples taken from the bioreactor on the corresponding DPI. It does not indicate an additional half a day (12 h) of infection. Due to this confusion, the process eventually moved to hours post infection (HPI) nomenclature. Data within this manuscript is presented as it was originally collected in DPI. This results in a window of optimal harvest timing (peak titer) typically ranging from 46–53 HPI, which may be originally represented as either 2 DPI or 2.5 DPI.

2.10. Titer determination by plaque assay

The plaque assay is used for determining the content of rVSVΔG-SARS-CoV-2 by infection of host Vero cells and subsequent quantitation

of the number of plaque forming units per milliliter (PFU/mL). Briefly, a dilute solution of virus is applied to a confluent monolayer of host cells then overlaid with a viscous medium to prevent the convective spread of virus. An inoculum volume of 150 μL is added to Vero plated 24-well plates using four two-fold serial dilutions. The virus is left to adsorb for one hour at 37 °C and the infected culture is then incubated for approximately 44 h. The virus infected cells lyse and spread the infection to adjacent cells where the infection-to-lysis cycle repeats. The infected cell area will create a plaque, an area of cell death surrounded by cells, which are visualized through staining with crystal violet and are counted manually. The number of infectious virus particles in the original solution is estimated based on the number of plaques observed by multiplying the number of plaques by the dilution of the virus and 6.7 to adjust for 1 mL. Virus content is reported in PFU/mL. For each sample, one vial is received for each run and each vial is diluted once per run. For a valid titer calculation result, the geometric mean of all valid titers from all dilutions on 24-well plates within 5–70 plaque is reported. A positive control is added with each run and must pass acceptance criteria for a valid run.

2.11. Titer determination by μPlaque assay

Viral potency measurements were determined using a μPlaque method, an automated, miniaturized plaque assay, where formations of viral plaques are grown and counted. Vero cells were seeded in DMEM/High Glucose (2% FBS, 1% Pen Strep) at 40,000 cells per well in 96-well tissue culture microplates (Corning). Cells were allowed to attach overnight and incubated at 37 °C, 5% pCO_2, >90% relative humidity. Media was aspirated from tissue culture plate prior to infection. Viral inoculum (serially diluted virus) was transferred to the 96-well plate containing a confluent cell layer (target >90% confluence) and incubated at 37 °C, 5% pCO_2, >90% relative humidity. After 4-hour viral attachment, overlay medium comprised of DMEM/High Glucose (10% FBS, 1% Pen Strep, 1% Methyl Cellulose (Fisher Chemical) was added to inhibit viral secretion and spread and incubated at 37 °C, 5% pCO_2, >90% relative humidity. Following an additional 24-hour infection incubation, overlay medium was aspirated from the plate for cell fixation using 3.7% formaldehyde (Sigma) for 30 min at ambient temperature. Formaldehyde was aspirated from the plate and phosphate buffered saline (Cytiva) was added prior to staining and held at ambient temperature. Cells were permeabilized with 0.5% Triton for 20 min at ambient temperature. Permeabilization buffer was aspirated from the plate and simultaneously blocked with 0.1% Tween-20 and 1% Bovine Serum Albumin in PBS (Teknova) and stained with 1 μg/mL Hoechst 33,342 for nuclear DNA (Thermo Fisher) for 30 min at ambient temperature. Hoechst stain aspirated and cells immunostained with 1 μg/mL SARS-CoV-2 Spike Neutralizing Rabbit Monoclonal Antibody (Sino Biological) and incubated for 1 hour at ambient temperature. The plate was washed with 0.1% Tween-20 in PBS (Sigma) for three cycles and then primary SARS-CoV-2 antibody conjugated to a 1:100 diluted Alexa Fluor 488 AffiniPure Donkey Anti-Rabbit IgG (Jackson Immunoresearch) and incubated for 1 hour at ambient temperature. Then the plate was washed with 0.1% Tween-20 in PBS (Sigma) for three cycles and PBS was added to plate following immunostaining. Automated image acquisition was completed using a Perkin Elmer EnSight reader, and plaques were partitioned and counted using Kaleido software. Plaque titer was calculated using the equation as described

$$Plaque\ Titer = \frac{PFU}{Inoculum\ Vol} xDF$$

where PFU is equivalent to the plaque forming units and DF is the dilution factor. The μPlaque assay allows for high-throughput titer analysis and we used the method to determine for virus titers for all experiments at 2 and 3 L scales.

2.12. Statistical analysis

JMP® software version 15.2 (SAS, NC) was used for the generation of design of experiments (DOE) and statistical analysis presented throughout the manuscript. Experimental data was used to create a linear model fit to the response variable, which was either cell growth (viable cells/mL) (vc/mL) or titer (Plaque Forming Unit/mL) (PFU/mL). For the 3 L bioreactors DOE study, the 15-run experiment, with D-optimality criterion selected, was used to design the DOE on virus production optimization. This design allows for the estimation of pH and temperature, two-way interaction, and the quadratic effect of temperature. Pair-wise analysis was performed between experimental conditions and control baseline process using the Tukey's HSD test when comparing across three or more levels and Student's *t*-test when comparing across two-levels.

3. Results and discussion

3.1. Optimization for rVSV-SARS-CoV-2 production in 3 L bioreactors

Temperature and pH are two critical parameters that need to be controlled during the virus production phase of the process. To optimize rVSV-SARS-CoV-2 production, we performed a Design of Experiment (DOE) study in 3 L bioreactors to study the impact of temperature and pH on virus production. We selected three temperature 32 °C, 34 °C and 37 °C and two pH set points 7.0 and 7.3 for the infection parameters DOE. Lowering temperature from 37 °C to 34 °C during infection has been reported to increase rVSV production in Vero cells [15]. The pH range was selected based on our previous experience with optimizing live virus vaccine production in Vero cells (unpublished data). Cell growth was compared between the conditions, and there was not a statistically significant difference in cell growth (data not shown). Fig. 1a shows the production of rVSV-SARS-CoV-2 for various infection conditions over time as measured by μPlaque. Infection temperature of 34 °C and pH 7.0 produced the maximum titer of 1.1e+7 PFU/mL at approximately 2.5 DPI compared to the other temperature and pH combinations. Similar to other studies, the maximum rVSV-SARS-CoV-2 production was achieved at 34 °C compared to 37 °C [26,27,15].

From this experiment we found that the effects of temperature ($p = 0.0102$), DPI ($p < 0\ 0.0001$), the interaction of pH and DPI ($p = 0.0009$), and the quadratic effect of DPI ($p < 0.0001$) were statistically significant (95% confidence). Note that although the effect of pH alone was not statistically significant, the effect of pH scored a p-value of 0.0532. Despite the main effect of pH not being truly statistically significant, it does show a trend that lower pH appears beneficial in terms of viral titer (Fig. 1b). Using this linear model, we can determine the optimal harvest time. Fig. 1b shows a linear model generated from the data that predicts an optimal pH of 7.0 and temperature of 34 °C with the optimal harvest timing for achieving peak potency at approximately 2.5 DPI.

3.2. Demonstration of optimal rVSV-SARS-CoV-2 production process in 50 L SUB

To ensure that the optimal infection temperature of 34 °C and pH 7.0 identified from the 3 L bioreactor DOE study would translate to large-scale bioreactors, we evaluated the optimal rVSV-SARS-CoV-2 production process at 50 L scale. Fig. 2 shows production of rVSV-SARS-CoV-2 at two different temperature and pH combinations in 50 L bioreactors. At lower temperature and pH combination of 34 °C and pH 7.0, virus production increased rapidly from 1 DPI to 2 DPI reaching a peak titer of 8.6e+6 PFU/mL while the higher temperature and pH condition of 37 °C and pH 7.3 only produced 2.8e+6 PFU/mL. Pair-wise comparison between the two groups showed there was not a statistically significant difference, but it approaches a p-value of 0.05 ($p = 0.0541$). When exponentiating the difference on the log scale, 0.6898 ln (PFU/mL), we find that there is on average a 2-fold difference between 34 °C, pH 7.0

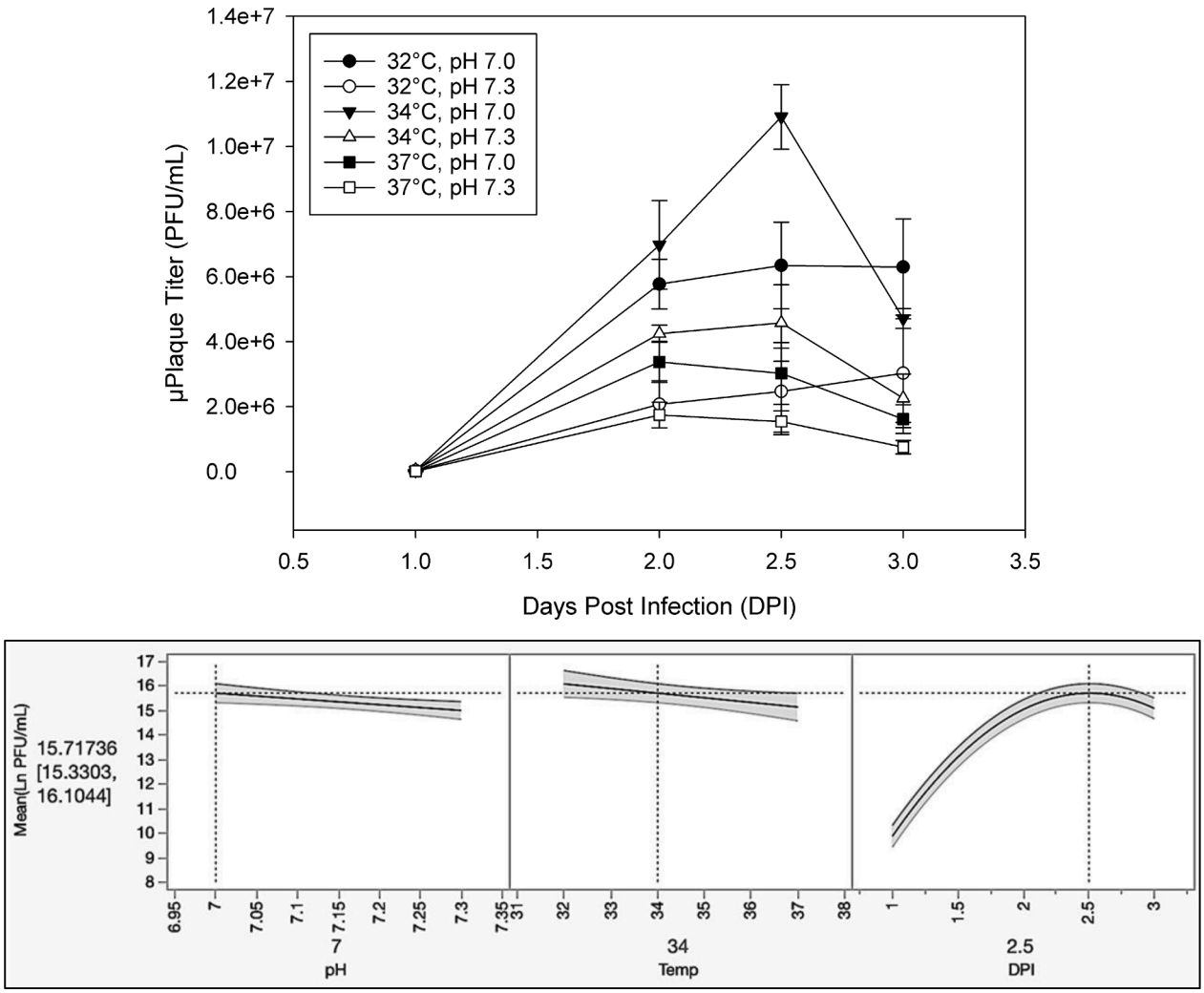

Fig. 1. a. Comparison of production of rVSV-SARS-CoV-2 at various infection conditions, with temperatures ranging from 32 °C to 37 °C and pH of either 7.0 or 7.3 in 3 L bioreactors. $N = 1$ for all conditions except 32 °C, pH 7.3 and 32 °C, pH 7.0 which have $n = 2$. Virus production titers measured by µPlaque (PFU/mL) are plotted against days post infection (DPI). Data represents means by condition, with at least 2 independent samples per bioreactor ± 1 standard deviation.
b. Linear model specifying optimal infection pH and temperature during virus production phase and harvest time. The model predicts that the optimal infection parameters are a pH of 7.0, a temperature of 34 °C, and a harvest time of approximately 2.5 days post-infection.

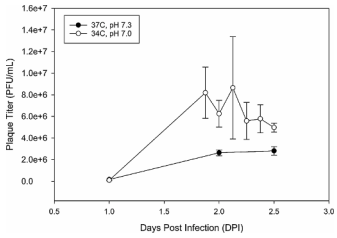

Fig. 2. Comparison of production of rVSV-SARS-CoV-2 at two different temperature and pH combinations: 34 °C/pH 7.0 ($n = 1$) and 37 °C/pH 7.3 ($n = 1$) in 50 L bioreactors. Virus production titers measured by Plaque (PFU/mL) are plotted against days post infection (DPI). Data represents the means of at least 3 independent samples per bioreactor ± 1 standard deviation.

and 37 °C, pH 7.3. This fold-difference constitutes a practically significant difference between processing conditions, and as such can be considered a meaningful processing difference. The dip in titer observed at 2 DPI in the 34 °C and pH 7.0 condition could be attributed to plaque assay variability or sample handling. These results confirmed the scalability and reproducibility of the optimal virus production temperature and pH identified from the 3 L bioreactor DOE study.

3.3. Scale-up production of rVSV-SARS-CoV-2 to 2000 L SUB

After establishing a large-scale process at 50 L scale and determining optimal operating conditions, the rVSV-SARS-CoV-2 N-stage production process was scaled-up to 500 L and 2000 L. Successful scale up from 50 L to 2000 L was enabled by developing a method to dispense large quantities of Cytodex 1 Gamma microcarriers in a closed system, increasing seeding cell density, scaling agitation rates, and modifying the pH control strategy.

The use of Cytodex 1 Gamma microcarriers was necessary to support large-scale bioreactor production. Heat-sterilized Cytodex 1 microcarriers were not an option for the 2000 L bioreactor process, since this would require the preparation of large volumes of hydrated microcarriers and sterilization. Large volumes of Cytodex 1 would need to be washed and heat sterilized prior to addition to the bioreactor. Cytodex 1 Gamma microcarriers are purchased gamma-irradiated and ready to use which is better for large-scale manufacturing processes. Since the manufacturer does not guarantee the weight of microcarriers in each stock container, it was necessary to re-dispense microcarriers to ensure the weight was known. Open dispensing and weighing in a biosafety cabinet are avoided in GMP production to reduce contamination risk. To enhance aseptic control and process efficiency, we developed a closed

single use transfer method to weigh and aliquot Cytodex 1 Gamma microcarriers into 2 L PETG bottles. Microcarriers were then added to the bioreactor as dry powder, instead of hydrating them prior to addition. Cytodex 1 microcarrier solution must be prepared to the manufacturer's recommended maximum concentration of 25 g/L. At 2000 L scale, this would require multiple bottles of autoclaved microcarriers to be individually added to the bioreactor. Our dry dispense method with hydration inside the bioreactor was significantly more efficient because the dry microcarriers could be prepared in two 2 L PETG bottles.

Static cell growth provided sufficient cells to inoculate 3 L bioreactor experiments. However, to generate a robust method to scale up instead of scaling out, an N-1 step was developed for cell inoculation at the 50, 500, and 2000 L scale. Harvesting cells from N-1 bioreactor required *in-situ* cell detachment from microcarriers which could affect cell recovery, viability, and functionality. Detachment and reattachment of Vero cells to microcarriers is challenging and poses a major problem for process scale up [28]. Cells harvested from the N-1 static cell growth have higher growth rate in bioreactors when compared to cells harvested from N-1 bioreactors (unpublished data). To achieve higher cell densities at infection, we increased the seeding cell density to 2.2e+4 viable cells/cm^2 for 50 to 2000 L scales. Increasing the seeding cell density to 2.2e+4 viable cells/cm^2 showed growth that was comparable to bioreactors inoculated at 1.3e+4 vc/cm^2 from N-1 static cell growth (data not shown). Cells harvested from a 250 L N-1 could support a maximum seeding density of 2.2e+4 vc/cm^2 in a 2000 L N-stage bioreactor with 1 g/L Cytodex 1.

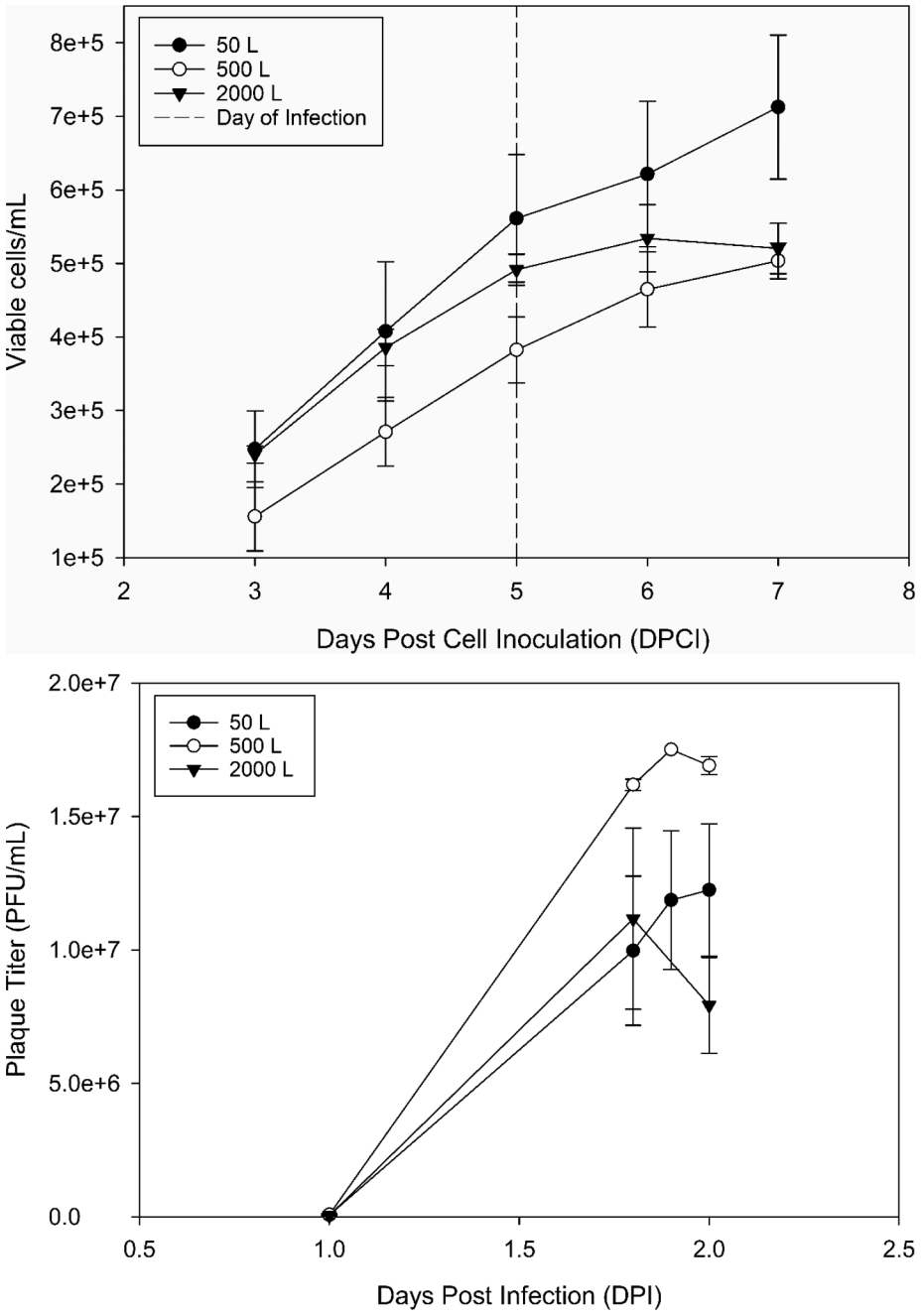

Fig. 3. **a**. Comparison of Vero cell growth in 50 L ($n = 4$), 500 L ($n = 2$) and 2000 L ($n = 1$) bioreactors. Cell growth expressed as vc/mL is plotted against days post cell inoculation (DPCI). Data represents means by scale, with at least 4 independent samples per bioreactor ± 1 standard deviation.
b. Production of rVSV-SARS-CoV-2 in 50 L ($n = 4$), 500 L ($n = 2$) and 2000 L ($n = 1$) bioreactors. Virus production titers measured by Plaque (PFU/mL) are plotted against days post infection (DPI). Data represents means by scale, with at least 3 independent samples per bioreactor ± 1 standard deviation.

When scaling up from 50 to 2000 L, cell culture conditions, including pH, temperature, DO setpoints and bioreactor bag specifications, including impeller turndown ratio and bag film were maintained the same. However, agitation rates needed to be scaled to ensure that the cells were subject to the same mixing conditions. The ideal agitation rate was determined empirically in 50 L bioreactors, and this was used to calculate the power per unit volume. This power per unit volume was used to calculate the agitation rates at 500 L and 2000 L scales. Keeping the power per unit volume constant across different scales ensured that the microcarriers were uniformly suspended and the cells were not subject to too much shear stress.

Culture sparging can be detrimental to Vero cells grown in serum free conditions [23]. Thus, gas addition via sparge must be avoided during the early growth phase to promote cell attachment and spreading. The gas demand in the culture, and the volume of the bioreactor needed to be considered when designing the aeration strategy at larger scales. Larger bioreactors require more gas addition via sparge because the headspace to liquid ratio is lower. Oxygen addition was not needed at any scale until after the attachment period of approximately ~1.5 days because the culture had low oxygen demand up to that point.

We use two-sided pH control where no Na_2CO_3 or CO_2 addition occurs while the pH process value is within ± 0.05 of the setpoint. This results in a constant addition of CO_2 during early growth to balance media off-gassing and stabilize the pH process value at the top of the specified range. At 50 L scale this strategy works since CO_2 addition is only through headspace; however, in the 2000 L bioreactor, CO_2 sparging must be used to sufficiently control pH. For 2000 L scale, we forced the pH to the setpoint prior to inoculating the cells. After cell inoculation, the pH drifted from setpoint to the top of the range, and then CO_2 addition via sparge was initiated. This process took approximately 1.5 days and ensured that no sparge was added to the bioreactor during the attachment period. The 500 L scale can utilize either the 50 L or 2000 L strategy.

Fig. 3a shows cell growth across 50, 500, and 2000 L scales, with 50 L showing the highest cell growth. Pair-wise analysis shows the difference in cell growth was statistically significant between scales ($p < 0.0007$). At 5 DPCI, cell density reached 5.6e+5, 3.8e+5 and 4.9e+5 vc/mL in 50 L, 500 L and 2000 L bioreactor, respectively. It is interesting that we did not observe a decrease in Vero cell density after infection with rVSV as has been reported previously by [15]. During our work, cell density continued to increase after virus infection, reaching 7.1e+5, 5.2e+5 and 5.0e+5 vc/mL at 7 DPCI. One possible explanation could be that Kiesslich et al., infected Vero cells at MOI of 0.01 and we infected at a lower MOI of 0.001 which might cause a slower decrease in viable cell density. As shown in Fig. 3a, post-infection, cells growing in 500 L and 2000 L bioreactors began to plateau but cells in 50 L bioreactor continued to grow, reaching a peak of 7.0e+5 vc/mL at 7 DPCI. MX operations at the 500 L and 2000 L scales, including microcarrier settling, decant, and post-addition media warming take longer than at the 50 L scale and this could affect how cells grow post-MX.

Higher peak cell density across scales did not correlate to higher titer. The highest cell growth was seen in 50 L bioreactors; however, the highest virus production titer was seen at the 500 L scale, as shown in Fig. 3b. All three scales were able to produce titers greater than the target of 1.0e+7 PFU/mL. Peak titers achieved on ~ 2 DPI were 1.2e+7, 1.8e+7 1.1e+7 PFU/mL for 50 L, 500 L and 2000 L bioreactors, respectively. The decrease in titer at 2 DPI for the 2000 L bioreactor was most likely due to sample processing or plaque assay variability. Based on the peak virus titers achieved at approximately 2 DPI for 50 L and 500 L scales, 2 DPI was designated as the fixed harvest timepoint across all three scales.

3.4. Process intensification for rVSV-SARS-CoV-2 production

In order to further optimize and understand the true limit of viral production within our bioreactor system, we compared rVSV-SARS-CoV-2 production at various Cytodex 1 concentrations in 2 L bioreactors. To remove cell growth phase as a confounding factor, cells were grown for 4 days in the N-1 bioreactor. On 4 DPCI, a suspension of fully confluent cells grown on Cytodex 1 were removed from the N-1 bioreactor and concentrated or diluted to achieve the test microcarrier concentrations (1, 2, or 3 g/L) using the same media, VP-SFM. Once the cells and microcarrier suspensions were diluted or concentrated appropriately, each 2 L bioreactor was equilibrated to growth process parameters, temperature of 37 °C and pH of 7.3, prior to infection. Cell counts were performed to confirm the appropriate cell density was achieved and for the MOI calculation.

The 2 g/L Cytodex 1 condition had the same microcarrier concentration as the N-1 bioreactor and required the least manipulation prior to transfer into the 2 L bioreactors. On 4 DPCI, cell density for 2 g/L Cytodex 1 condition was 9.2e+5 vc/mL. Based on that cell density, we would expect theoretical cell densities of 4.63e+5 vc/mL for 1 g/L and 1.39e+6 vc/mL for 3 g/L Cytodex 1. The actual cell density for 1 g/L was 4.74e+5 vc/mL, but the mean cell density for two bioreactors at 3 g/L was 2.08e+6 vc/mL, which was higher than the expected value. It's likely that the two 3 g/L bioreactors received higher actual volumes of cell suspension than the calculated amount.

After bioreactors stabilized at growth temperature and pH set points, each bioreactor was infected with an MOI of 0.001 PFU/vc based on the viable cell density of the respective bioreactor. After virus addition, temperature and pH set points were changed to infection parameters of 34 °C and 7.0, respectively. As seen in Fig. 4a, viable cell densities peaked at 6.3e+5, 1.2e+6, and 2.7e+6 vc/mL for 1, 2 and 3 g/L Cytodex 1 respectively. Pair-wise comparisons between 2 g/L or 3 g/L and the 1 g/L Cytodex 1 baseline condition shows the difference in cell growth was statistically significant for each comparison ($p < 0.0001$).

Fig. 4b shows progression of rVSV-SARS-CoV-2 production over time as determined by μPlaque. Peak infectious titers reached 2.9e+6, 1.0e+7, and 2.2e+7 PFU/mL for 1, 2, and 3 g/L Cytodex 1 respectively. Under these experimental conditions, Vero cells grown on a concentration of 3 g/L Cytodex 1 produced the highest titer of rVSV-SARS-CoV-2. Compared to 1 g/L, the 3 g/L Cytodex 1 produced a 7-fold increase in virus production. The pair-wise comparison between Cytodex 1 concentrations showed that difference in titer between 1 g/L and 3 g/L Cytodex 1 was statistically significant ($p = 0.0028$), but surprisingly 1 g/L compared to 2 g/L was not statistically significant ($p = 0.2812$) despite a nearly 3-fold higher titer at 2 g/L; this was attributed to variability of the μPlaque assay.

To generate additional data for this process intensification, a comparison of 1 and 2 g/L Cytodex 1 was tested at the 50 L scale. We chose the 2 g/L, and not 3 g/L Cytodex 1 concentration to evaluate at the 50 L scale due to limitation of the N-1 cell harvest yield. As expected, the 2 g/L Cytodex 1 condition supported higher cell density and rVSV-SARS-CoV-2 titer. As shown in Fig. 5a, the 2 g/L bioreactor reached a cell density of 6.6e+5 compared to 5.7e+5 vc/mL at 1 g/L at 5 DPCI. Pair-wise analysis between the two Cytodex 1 concentrations showed the difference in cell growth was statistically significant ($p = 0.0002$). Fig. 6a and 6b show that the 2 g/L bioreactor consumed more of both glucose and L-glutamine and required a glucose feed on 4 DPCI. As shown in Fig. 6c, the 2 g/L bioreactor produced more lactate during growth but produced comparable lactate to the 1 g/L condition during infection. These metabolite results are consistent with expectations for higher cell growth.

Increased cell growth translated to higher virus titer peaks in the 2 g/L condition (Fig. 5b). The maximum titer reached was 2.2e+7 PFU/mL at 2 DPI in the 2 g/L Cytodex 1 bioreactor, compared to 1.1e+7 PFU/mL in the 1 g/L bioreactor. This represents a 2-fold increase in virus production. There was a statistically significant difference ($p = 0.0012$) between the two conditions. These data agree with results at the 2 L scale, demonstrating a 2-fold increase in titers could be achieved through increases in Cytodex 1 concentration.

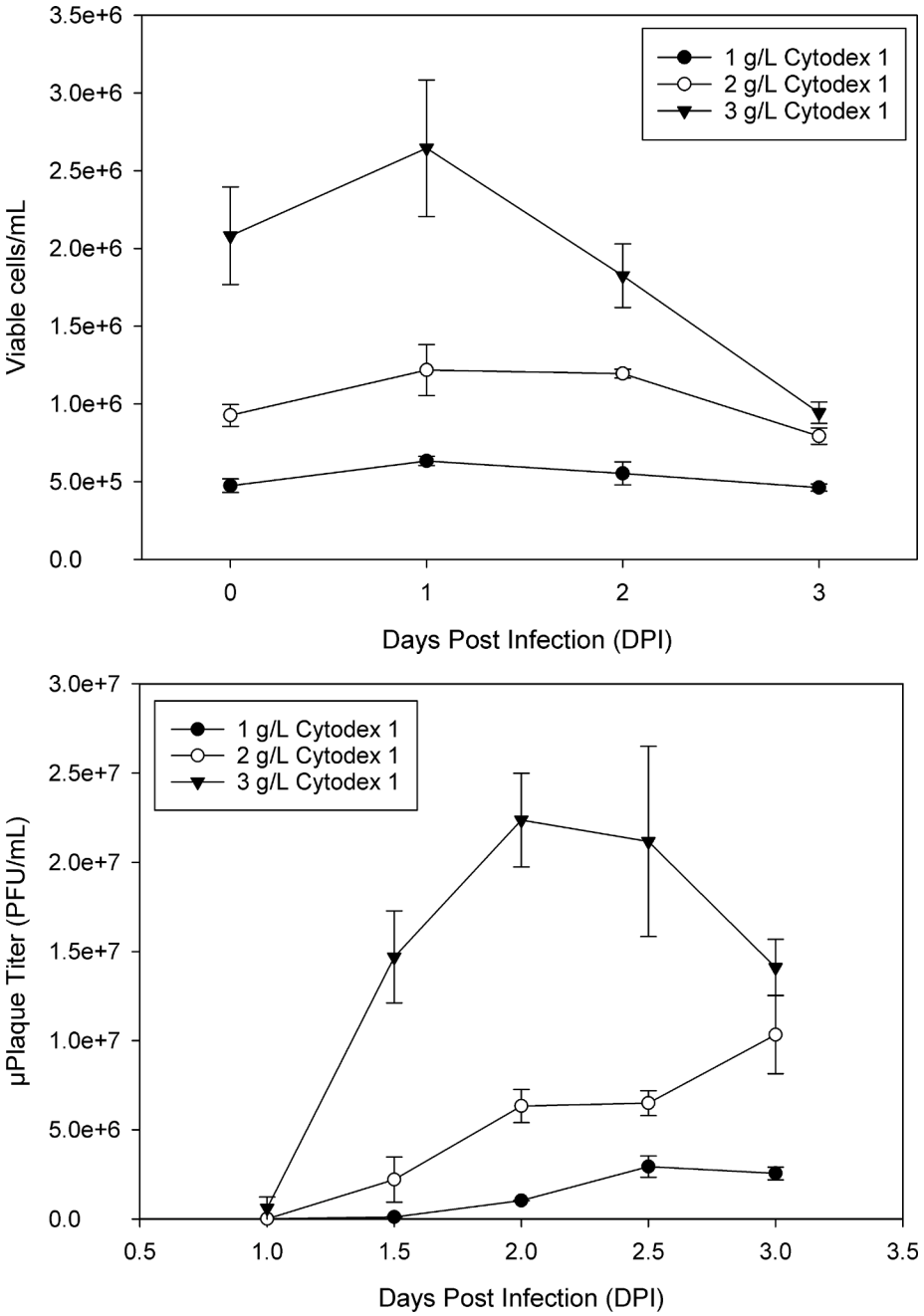

Fig. 4. **a**. Comparison of viable cell density for 1 g/L ($n = 1$), 2 g/L ($n = 2$), and 3 g/L ($n = 2$) Cytodex 1 in 2 L bioreactors. Cell growth expressed as vc/mL is plotted against days post cell inoculation (DPCI). Data represents means by condition, with at least 2 independent samples per bioreactor ± 1 standard deviation. **b**. Comparison of µPlaque titers for 1 g/L ($n = 1$), 2 g/L ($n = 2$), and 3 g/L ($n = 2$) Cytodex 1 in 2 L bioreactors. Virus production titers measured by µPlaque (PFU/mL) are plotted against days post infection (DPI). Data represents means by condition, with at least 2 independent samples per bioreactor ± 1 standard deviation.

3.5. Removal of media exchange (MX)

To simplify the large-scale production process, we evaluated the removal of MX and examined process impacts on virus production. At 2000 L scale, the MX step can take up to 3 h to complete. Due to the relatively short duration of the virus production phase of approximately two days and the absence of unique production media, removal of the MX step would have significant impact on manufacturing hours as well as material and resource costs. Six 3 L glass bioreactors were split into two arms, $n = 3$ each: control (with MX) vs. no MX and were monitored for virus production by µPlaque over the infection phase. As shown in Fig. 7a, cell growth was comparable between the two conditions, there was no statistically significant difference between the two groups ($p = 0.4578$). Cell density for both conditions continued to increase after virus infection. The MX condition reached a peak cell density of 5.8e+5 vc/mL at 7 DPCI (2 days post-infection) whereas no MX reached a peak cell density of 6.3e+5 vc/mL at 6 DPCI (1 day post-infection). During the virus production phase, no MX resulted in faster decline in viable cell density compared to control condition.

Surprisingly, there was no detrimental impact to virus production as a result of no MX and, in fact, not performing MX increased virus production. As indicated in Fig. 7b, bioreactors that did not have MX had nearly a three-fold increase in virus production compared to the MX condition in peak virus titer on 2 DPI (2.9e+7 PFU/mL vs 9.8e+6 PFU/mL); this increase in titer was statistically significant ($p = 0.0040$).

Similarly at the 50 L scale, an optimization study was performed to

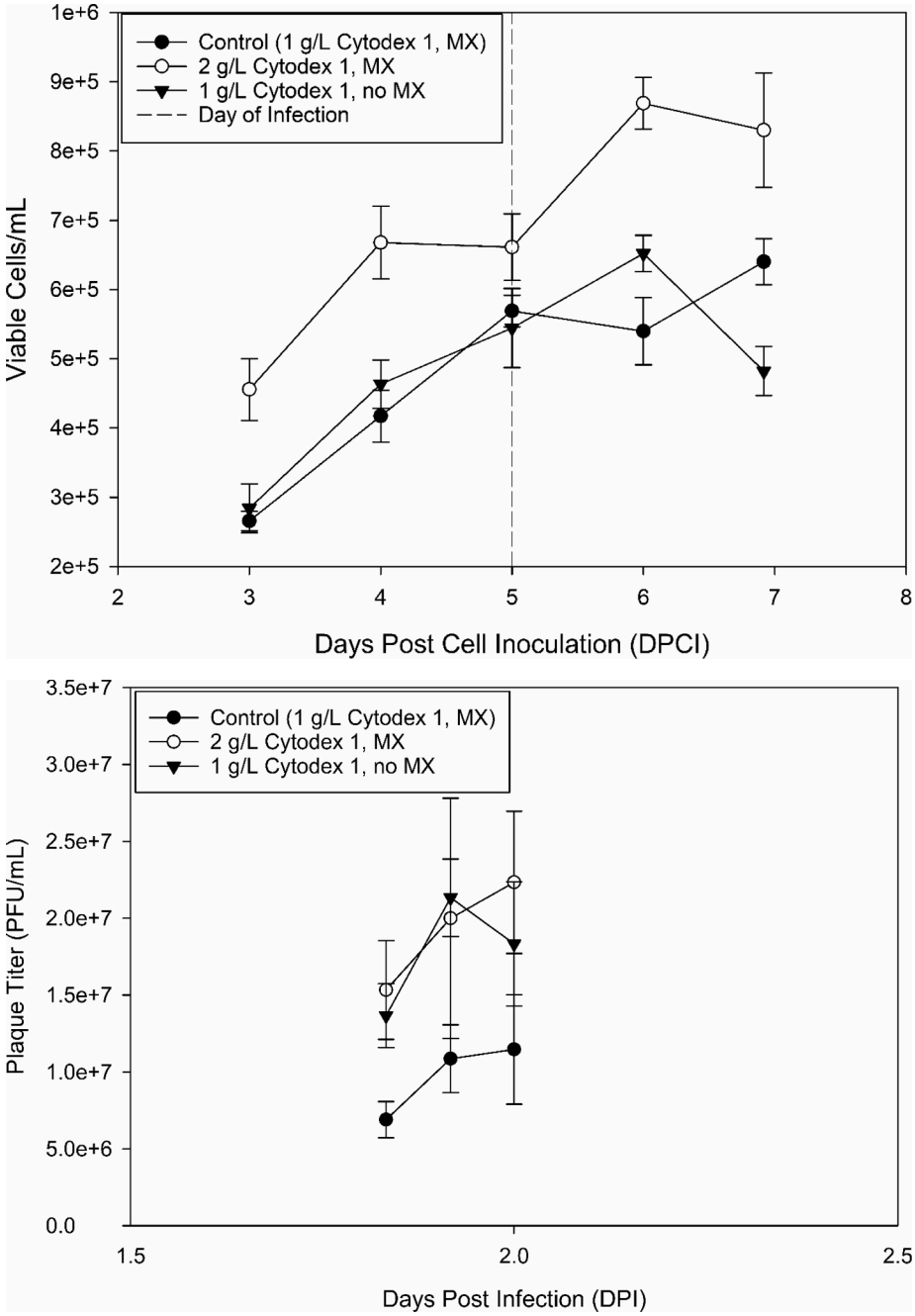

Fig. 5. **a**. Vero cells growth in 50 L bioreactors with 1 g/L Cytodex 1 with MX ($n = 1$), 2 g/L Cytodex 1 ($n = 1$), and 1 g/L Cytodex 1 without MX ($n = 1$). Cell growth expressed as vc/mL is plotted against days post cell inoculation (DPCI). Data represents the means of at least 4 independent samples per bioreactor ± 1 standard deviation.
b. Production of rVSV-SARS-CoV-2 in 50 L bioreactors with 1 g/L Cytodex 1 with MX ($n = 1$), 2 g/L Cytodex 1 ($n = 1$), and 1 g/L Cytodex 1 without MX ($n = 1$). Virus production titers measured by Plaque (PFU/mL) are plotted against days post infection (DPI). Data represents the means of at least 3 independent samples per bioreactor ± 1 standard deviation.

evaluate the removal of MX. As shown in Fig. 5a, on 5 DPCI, cell densities were comparable between the 1 g/L control and 1 g/L with no MX conditions. Removing the MX step did not cause a significant difference to cell growth ($p = 0.8345$). Fig. 6a-c show the L-glutamine, glucose, and lactate concentrations in each of the bioreactors. During growth, the no MX condition trended very closely to the control. Glucose and L-glutamine were not limited in the no MX condition, staying above 5 mM and 1 mM respectively. Lactate concentration was higher in the no MX condition during the infection phase because waste was not removed with the MX step. The no MX condition generated higher titers than the control. The no MX condition generated a maximum titer of 1.8e+7 PFU/mL compared to 1.1e+7 PFU/mL with MX on 2 DPI (Fig. 5b). The pair-wise analysis between the control and no MX condition showed there was a statistically significant difference ($p = 0.0019$) in virus production between the two conditions, providing further confirmation that future process optimization for the 2000 L bioreactor could be achieved by eliminating the MX step.

The increase in virus production in the no MX condition is likely due to healthier and stress-free cells. MX required microcarriers to settle for an extended period of time, which might limit the oxygen and nutrients available to cells. In addition, during the settling period, cells and microcarriers pack on top of each other, which might generate

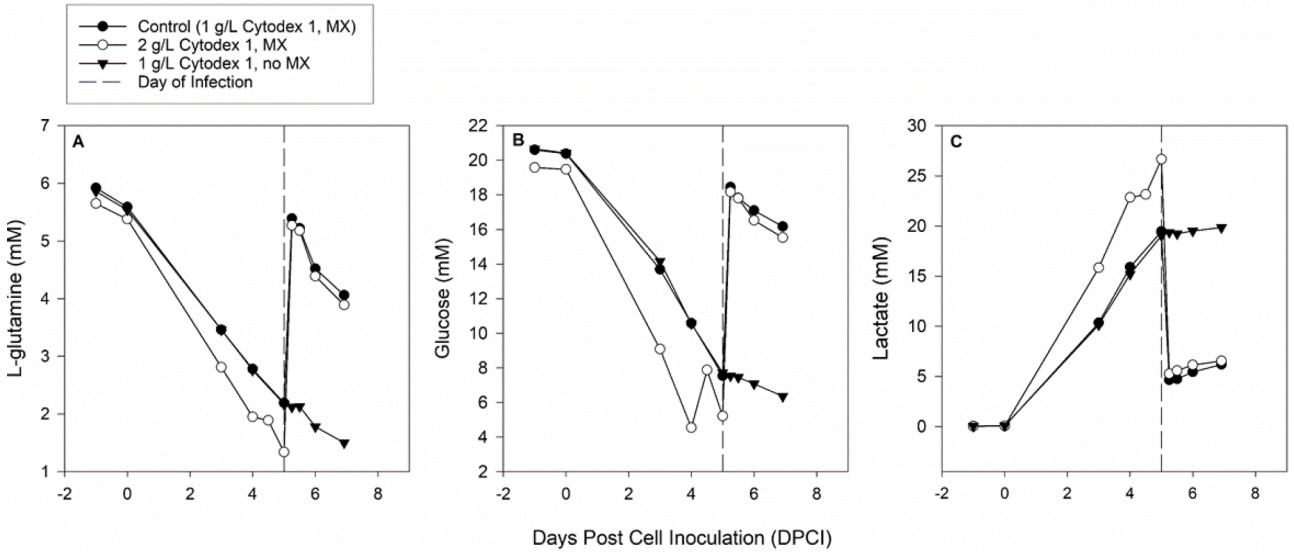

Fig. 6. L-glutamine (A), glucose (B) and lactate (C) concentrations in 50 L bioreactors with 1 g/L Cytodex 1 with MX ($n = 1$), 2 g/L Cytodex 1 ($n = 1$), and 1 g/L Cytodex 1 without MX ($n = 1$). Metabolite concentrations measured by Nova Bioprofile Flex 2 are plotted against days post cell inoculation (DPCI). Data represents one sample reading per bioreactor.

additional physical stress for cells. It is plausible that the combination of physiological and physical stress experienced by cells during the MX step might result in lower virus production compared to the no MX process.

Other possible reasons for the increase in virus production are changes in host cell metabolism and innate immune signaling. It is well established that viral infection induces changes in both host cell metabolism and immune signaling pathways to favor viral replication [29, 30]. One major difference present in the no MX condition is that lactate levels remain elevated, as shown in Fig. 6c, rather than this metabolic by-product being removed in the spent media during MX. This increased lactate concentration at the start of infection might be a key contributor to the observed titer increase. It has been documented that viral infection mimics that of cancer and tumor progression with exhibition of the Warburg effect [30]. Lactate, as an acidic species, can affect cellular pH dynamics. Dysregulation of pH within cancer cells has been shown to have an effect on cell proliferation and cell survival by limiting apoptosis [31–33]. In addition to its role in cell metabolism, lactate has also been implicated in the Rig-I like receptor (RLR) immune signaling pathways. Zhang et al. established that lactate binds to mitochondrial antiviral-signaling protein (MAVS) to inhibit RLR activation and subsequent interferon (IFN) production [34]. Although Vero cells lack the ability to produce IFN [35], there might be other IFN-independent innate immune pathways that lactate is modulating. It has been shown that VSV infection modulates many genes even in the absence of IFN signaling [36]. It is plausible that with its role in both cell metabolism and innate immune signaling, increased initial levels of lactate in bioreactors without MX have “primed” the cells for a favorable viral replication environment. The removal of the MX step prior to infection has also been successfully implemented for rabies and influenza without impacting virus production [37,23]. Overall, we demonstrated a two-fold increase in viral titers through either microcarriers intensification or removal of the MX step.

In response to the outbreak of COVID-19, we leveraged single use technologies to rapidly develop a scalable, GMP-compliant closed manufacturing process for rVSV-SARS-CoV-2. Utilizing single use components enabled us to accelerate the process development timeline and enhance process flexibility and efficiency. From static cell growth to large-scale bioreactor operations, utilizing single use components improved aseptic control and turn-around time. The 2000 L production process for rVSV-SARS-CoV-2 was completely closed except for the initial vials thaw step. Closed processing not only minimizes contamination risk but also prevents potential exposure to infectious organisms. Sterile welders and aseptic connectors were used for processing and material transfer and eliminating open aseptic processing, thus reducing contamination and exposure risk. SUBs enabled experiments to be set up quickly; they could be taken down and set up for the next experiment during the same day, allowing for rapid implementation of process changes and demonstration of process iterations. From a manufacturing perspective, utilizing single use components also helped to accelerate timeline of bringing the vaccine to clinic. Installation and commissioning of a SUB in a manufacturing facility are easy and fast. Furthermore, cleaning validation for new product is greatly reduced when single use components are used.

4. Conclusion

In this study, a GMP-compliant, closed, and disposable microcarrier bioreactor manufacturing process was developed for a rVSV-SARS-CoV-2 vaccine candidate. To determine the optimal condition for virus production, a DOE study was performed in 3 L bioreactors to evaluate the impact of temperature and pH on rVSV-SARS-CoV-2 production. From this study, the optimal infection temperature of 34.0 °C and pH 7.0 were identified and successfully applied and scaled up to a 2000 L bioreactor, producing a maximum titer of ~1e+7 PFU/mL. To our knowledge, this is the first work that describes the development of an industrial scale closed fully disposable microcarrier manufacturing process for a live virus vaccine. Further process intensification, including increasing microcarrier concentration to 2 g/L and eliminating the MX step prior to infection helped to increase virus productivity in 50 L bioreactor by ~2 fold. Future experiments should evaluate serial microcarriers cell passaging or the intensification of N-1 bioreactor step to produce sufficient cells to support a 2 g/L microcarriers process at 2000 L scale.

CRediT authorship contribution statement

Christopher Ton: Conceptualization, Supervision, Methodology, Investigation, Data curation, Writing – original draft, Writing – review & editing. **Victoria Stabile:** Conceptualization, Methodology, Investigation, Data curation, Writing – original draft, Writing – review & editing. **Elizabeth Carey:** Conceptualization, Methodology, Investigation, Data curation, Writing – original draft, Writing – review & editing. **Adam**

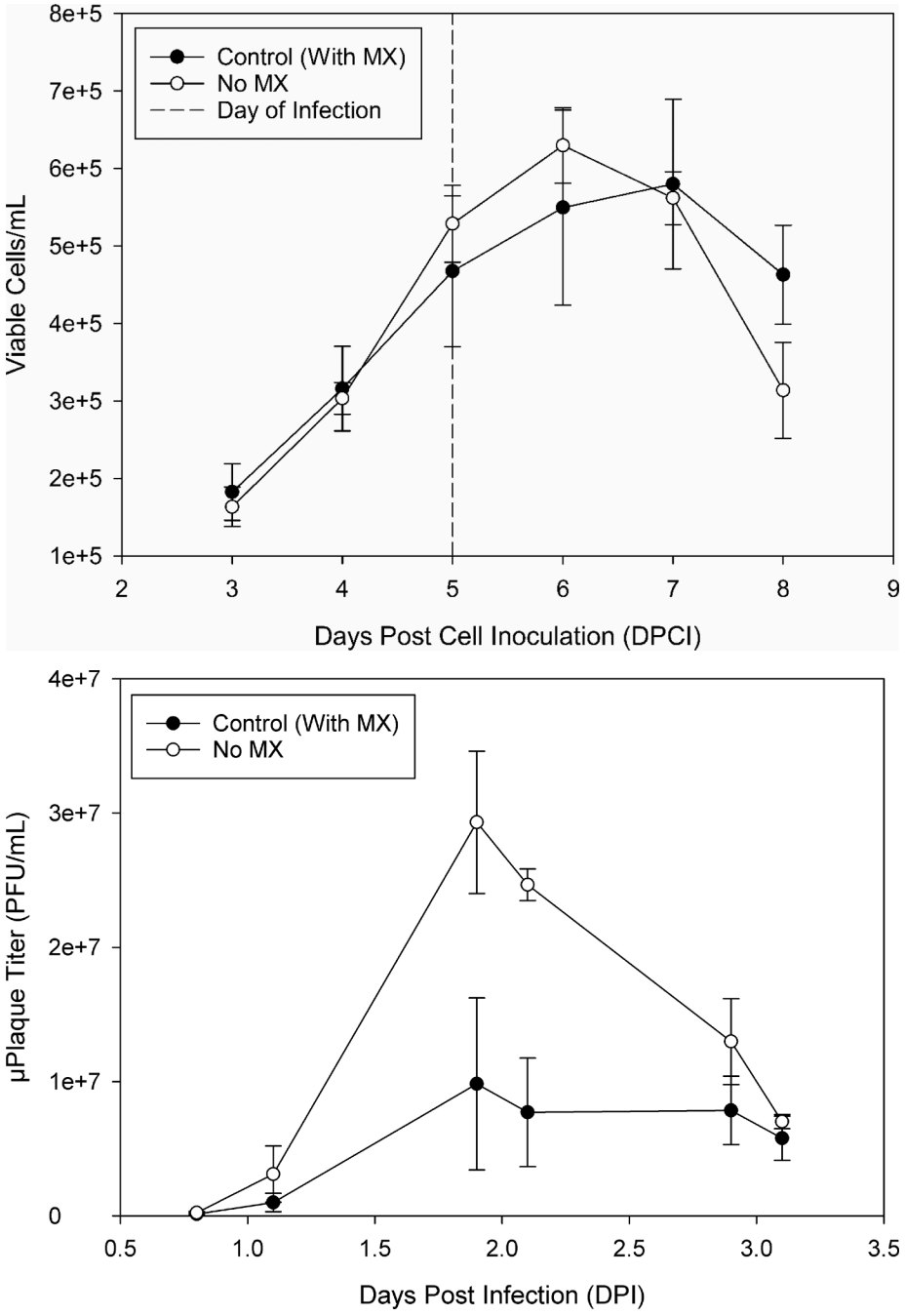

Fig. 7. a. Head-to-head comparison of Vero cell growth in 3 L bioreactors between with MX ($n = 3$) and without MX ($n = 3$) conditions. Cell growth expressed as vc/mL is plotted against days post cell inoculation (DPCI). Data represents the means by condition, with at least 2 independent samples per bioreactor ± 1 standard deviation.

b. Production of rVSV-SARS-CoV-2 with ($n = 3$) or without MX ($n = 3$) in 3 L bioreactors as measured by µPlaque. Virus production titers measured by µPlaque (PFU/mL) are plotted against days post infection (DPI). Data represents means by condition, with at least 2 independent samples per bioreactor ± 1 standard deviation.

Maraikar: Conceptualization, Methodology, Investigation, Data curation, Writing – original draft, Writing – review & editing. **Travis Whitmer:** Conceptualization, Methodology, Investigation, Data curation, Writing – original draft, Writing – review & editing. **Samantha Marrone:** Methodology, Investigation, Writing – original draft, Writing – review & editing, Resources. **Nelson Lee Afanador:** Investigation, Data curation. **Igor Zabrodin:** Investigation, Writing – review & editing. **Greeshma Manomohan:** Investigation, Writing – review & editing. **Melissa Whiteman:** Investigation, Writing – review & editing. **Carl Hofmann:** Investigation, Writing – review & editing.

Declaration of Competing Interest

The authors declare the following financial interests/personal relationships which may be considered as potential competing interests: Christopher Ton, Victoria Stabile, Elizabeth Carey, Adam Maraikar, Travis Whitmer, Samantha Marrone, Nelson Lee Afanador, Igor Zabrodin, Greeshma Manomohan, Melissa Whiteman, Carl Hofmann are/were employees of Merck Sharp & Dohme LLC, a subsidiary of Merck & Co., Inc., Rahway, NJ, USA, and may potentially own stock and/or hold stock options in Merck & Co., Inc., Rahway, NJ, USA. Greeshma Manomohan is currently an employee of GlaxoSmithKline plc.

Data availability

Data will be made available on request.

Acknowledgements

The authors wish to thank Doug Richardson for guidance and fruitful discussions during the development of this work. The authors are also grateful to Camilo Gutierrez, Josh McNeely, Daniel Salovich and James O'Connor for contributing to this study and to Katrina Feller, Kelsey Hines, Bryan McLaughlin, Nathan Kuster, Jenny Xu, Ashley Gruber for generating Plaque data. In addition, the authors wish to thank and acknowledge Matt Troutman and Kristine Kearns for generating µPlaque data. This project has been funded in part with Federal funds from the Department of Health and Human Services; Office of the Assistant Secretary for Preparedness and Response; Biomedical Advanced Research and Development Authority, under Contract No. HHSO100201600031C.

References

[1] J. Cui, F. Li, Z.L. Shi, Origin and evolution of pathogenic coronaviruses, Nat. Rev. Microbiol. 17 (3) (2019) 181–192, https://doi.org/10.1038/s41579-018-0118-9.
[2] J. Zhao, S. Zhao, J. Ou, J. Zhang, W. Lan, W. Guan, X. Wu, Y. Yan, W. Zhao, J. Wu, J. Chodosh, Q. Zhang, COVID-19: coronavirus vaccine development updates, Front. Immunol. 11 (2020), 602256, https://doi.org/10.3389/fimmu.2020.602256.
[3] Y. Shi, G. Wang, X.P. Cai, J.W. Deng, L. Zheng, H.H. Zhu, M. Zheng, B. Yang, Z. Chen, An overview of COVID-19, J Zhejiang Univ. Sci. B 21 (5) (2020) 343–360, https://doi.org/10.1631/jzus.B2000083.
[4] WHO Director-General's opening remarks at the media briefing on COVID19-March 2020.
[5] Saphire E. Ollmann, A vaccine against Ebola virus, Cell 181 (1) (2020) 6, https://doi.org/10.1016/j.cell.2020.03.011.
[6] S. Kiesslich, A.A. Kamen, Vero cell upstream bioprocess development for the production of viral vectors and vaccines, Biotechnol. Adv. 44 (2020), 107608, https://doi.org/10.1016/j.biotechadv.2020.107608.
[7] World Health Organization, Acceptability of cells substrates for production of biologicals, WHO Tech. Rep. Ser. 747 (1987) 5–24.
[8] World Health Organization, Requirements for continuous cell lines used for biological substances, WHO Tech. Rep. Ser. 745 (1987) 99–115.
[9] E. Vidor, C. Meschievitz, S. Plotkin, Fifteen years of experience with Vero-produced enhanced potency inactivated poliovirus vaccine, Pediatr. Infect. Dis. J. 16 (3) (1997) 312–322, https://doi.org/10.1097/00006454-199703000-00011.
[10] V.V. Emmerling, A. Pegel, E.G. Milian, A. Venereo-Sanchez, M. Kunz, J. Wegele, A. A. Kamen, S. Kochanek, M. Hoerer, Rational plasmid design and bioprocess optimization to enhance recombinant adeno-associated virus (AAV) productivity in mammalian cells, Biotechnol. J. 11 (2) (2016) 290–297, https://doi.org/10.1002/biot.201500176.
[11] A.D. Powers, B.A. Piras, R.K. Clark, T.D. Lockey, M.M. Meagher, Development and optimization of AAV hFIX particles by transient transfection in an iCELLis(®) fixed-bed bioreactor, Hum. Gene Ther. Methods 27 (3) (2016) 112–121, https://doi.org/10.1089/hgtb.2016.021.
[12] A.J. Valkama, H.M. Leinonen, E.M. Lipponen, V. Turkki, J. Malinen, T. Heikura, S. Ylä-Herttuala, H.P. Lesch, Optimization of lentiviral vector production for scale-up in fixed-bed bioreactor, Gene Ther. 25 (1) (2018) 39–46, https://doi.org/10.1038/gt.2017.91.
[13] A. McCarron, M. Donnelley, C. McIntyre, D. Parsons, Transient lentiviral vector production using a packed-bed bioreactor system, Hum. Gene Ther. Methods 30 (3) (2019) 93–101, https://doi.org/10.1089/hgtb.2019.038.
[14] D.M. Berrie, R.C. Waters, C. Montoya, A. Chatel, E.M. Vela, Development of a high-yield live-virus vaccine production platform using a novel fixed-bed bioreactor, Vaccine 38 (20) (2020) 3639–3645, https://doi.org/10.1016/j.vaccine.2020.03.041.
[15] S. Kiesslich, J.P. Vila-Chã Losa, J.F. Gélinas, A.A Kamen, Serum-free production of rVSV-ZEBOV in Vero cells: microcarrier bioreactor versus scale-X™ hydro fixed-bed, J. Biotechnol. 310 (2020) 32–39, https://doi.org/10.1016/j.jbiotec.2020.01.015.
[16] L.E. Gallo-Ramírez, A. Nikolay, Y. Genzel, U. Reichl, Bioreactor concepts for cell culture-based viral vaccine production, Expert Rev. Vaccines 14 (9) (2015) 1181–1195, https://doi.org/10.1586/14760584.2015.1067144.
[17] A.C. Silva, A. Roldão, A. Teixeira, P. Fernandes, M.F.Q. Sousa, P. Alves, Cell immobilization for the production of viral vaccines, Animal Cell Culture Volume 9 (2015) 541–563. Springer International.
[18] S. Rourou, M. Ben Zakkour, H. Kallel, Adaptation of Vero cells to suspension growth for rabies virus production in different serum free media, Vaccine 37 (47) (2019) 6987–6995, https://doi.org/10.1016/j.vaccine.2019.05.092.
[19] C.F. Shen, C. Guilbault, X. Li, S.M. Elahi, S. Ansorge, A. Kamen, R. Gilbert, Development of suspension adapted Vero cell culture process technology for production of viral vaccines, Vaccine 37 (47) (2019) 6996–7002, https://doi.org/10.1016/j.vaccine.2019.07.003.
[20] S. Kiesslich, G.N. Kim, C.F. Shen, C.Y. Kang, A.A. Kamen, Bioreactor production of rVSV-based vectors in Vero cell suspension cultures, Biotechnol. Bioeng. 118 (7) (2021) 2649–2659, https://doi.org/10.1002/bit.27785.
[21] P.N. Barrett, W. Mundt, O. Kistner, M.K. Howard, Vero cell platform in vaccine production: moving towards cell culture-based viral vaccines, Expert Rev. Vaccines 8 (5) (2009) 607–618, https://doi.org/10.1586/erv.09.19.
[22] D.A. Mattos, M.V. Silva, L.P. Gaspar, L.R. Castilho, Increasing Vero viable cell densities for yellow fever virus production in stirred-tank bioreactors using serum-free medium, Vaccine 33 (35) (2015) 4288–4291, https://doi.org/10.1016/j.vaccine.2015.04.050.
[23] S. Rourou, A. van der Ark, T. van der Velden, H. Kallel, A microcarrier cell culture process for propagating rabies virus in Vero cells grown in a stirred bioreactor under fully animal component free conditions, Vaccine 25 (19) (2007) 3879–3889, https://doi.org/10.1016/j.vaccine.2007.01.086.
[24] M. George, M. Farooq, T. Dang, B. Cortes, J. Liu, L. Maranga, Production of cell culture (MDCK) derived live attenuated influenza vaccine (LAIV) in a fully disposable platform process, Biotechnol. Bioeng. 106 (6) (2010) 906–917, https://doi.org/10.1002/bit.22753.
[25] A.S. Espeseth, M. Yuan, M. Citron, L. Reiserova, G. Morrow, A. Wilson, M. Horton, M. Rukhman, K. Kinek, F. Hou, S.L. Li, F. Li, Y. Choi, G. Heidecker, B. Luo, G. Wu, L. Zhang, E. Strable, J. DeStefano, S. Secore, …, C.L. Parks, Preclinical immunogenicity and efficacy of a candidate COVID-19 vaccine based on a vesicular stomatitis virus-SARS-CoV-2 chimera, EBioMedicine 82 (2022), 104203, https://doi.org/10.1016/j.ebiom.2022.104203.
[26] S.M. Elahi, C.F. Shen, R. Gilbert, Optimization of production of vesicular stomatitis virus (VSV) in suspension serum-free culture medium at high cell density, J. Biotechnol. 289 (2019) 144–149, https://doi.org/10.1016/j.jbiotec.2018.11.023.
[27] J.F. Gélinas, H. Azizi, S. Kiesslich, S. Lanthier, J. Perdersen, P.S. Chahal, S. Ansorge, G. Kobinger, R. Gilbert, A.A. Kamen, Production of rVSV-ZEBOV in serum-free suspension culture of HEK 293SF cells, Vaccine 37 (44) (2019) 6624–6632, https://doi.org/10.1016/j.vaccine.2019.09.044.
[28] M. Sousa, C. Fenge, J. Rupprecht, A. Tappe, G. Greller, P. Alves, M. Carrondo, A. Roldão, Process intensification for Peste des petites ruminants virus vaccine production, Vaccine 37 (47) (2019) 7041–7051, https://doi.org/10.1016/j.vaccine.2019.07.009.
[29] A. Alcami, U.H. Koszinowski, Viral mechanisms of immune evasion, Trends Microbiol. 8 (9) (2000) 410–418, https://doi.org/10.1016/s0966-842x(00)01830-8.
[30] S.K. Thaker, J. Ch'ng, H.R. Christofk, Viral hijacking of cellular metabolism, BMC Biol. 17 (1) (2019) 59, https://doi.org/10.1186/s12915-019-0678-9.
[31] S. Matsuyama, J. Llopis, Q.L. Deveraux, R.Y. Tsien, J.C. Reed, Changes in intramitochondrial and cytosolic pH: early events that modulate caspase activation during apoptosis, Nat. Cell Biol. 2 (6) (2000) 318–325, https://doi.org/10.1038/35014006.
[32] R. Pérez-Tomás, I. Pérez-Guillén, Lactate in the tumor microenvironment: an essential molecule in cancer progression and treatment, Cancers (Basel) 12 (11) (2020) 3244, https://doi.org/10.3390/cancers12113244.
[33] K.A. White, B.K. Grillo-Hill, D.L. Barber, Cancer cell behaviors mediated by dysregulated pH dynamics at a glance, J. Cell. Sci. 130 (4) (2017) 663–669, https://doi.org/10.1242/jcs.195297.
[34] W. Zhang, G. Wang, Z.G. Xu, H. Tu, F. Hu, J. Dai, Y. Chang, Y. Chen, Y. Lu, H. Zeng, Z. Cai, F. Han, C. Xu, G. Jin, L. Sun, B.S. Pan, S.W. Lai, C.C. Hsu, J. Xu, Z.Z. Chen, …, H.K. Lin, Lactate is a natural suppressor of RLR signaling by targeting MAVS, Cell 178 (1) (2019) 176–189, https://doi.org/10.1016/j.cell.2019.05.003, e15.
[35] J. Desmyter, J.L. Melnick, W.E. Rawls, Defectiveness of interferon production and of rubella virus interference in a line of African green monkey kidney cells (Vero), J. Virol. 2 (10) (1968) 955–961, https://doi.org/10.1128/JVI.2.10.955-961.1968.
[36] A.R. Mishra, S.N. Byrareddy, D. Nayak, IFN-i independent antiviral immune response to vesicular stomatitis virus challenge in mouse brain, Vaccines (Basel) 8 (2) (2020) 326, https://doi.org/10.3390/vaccines8020326.
[37] Y. Genzel, M. Fischer, U. Reichl, Serum-free influenza virus production avoiding washing steps and medium exchange in large-scale microcarrier culture, Vaccine 24 (16) (2006) 3261–3272, https://doi.org/10.1016/j.vaccine.2006.01.019.

Further readings

[1] M. Garbutt, R. Liebscher, V. Wahl-Jensen, S. Jones, P. Möller, R. Wagner, V. Volchkov, H.D. Klenk, H. Feldmann, U. Ströher, Properties of replication-competent vesicular stomatitis virus vectors expressing glycoproteins of filoviruses and arenaviruses, J. Virol. 78 (10) (2004) 5458–5465, https://doi.org/10.1128/jvi.78.10.5458-5465.2004.
[2] J. Harcourt, A. Tamin, X. Lu, S. Kamili, S.K. Sakthivel, J. Murray, K. Queen, Y. Tao, C.R. Paden, J. Zhang, Y. Li, A. Uehara, H. Wang, C. Goldsmith, H.A. Bullock, L. Wang, B. Whitaker, B. Lynch, R. Gautam, C. Schindewolf, N.J. Thornburg, Severe acute respiratory syndrome coronavirus 2 from patient with coronavirus disease,

United States, Emerging Infect. Dis. 26 (6) (2020) 1266–1273, https://doi.org/10.3201/eid2606.200516.

[3] S. Rabinovich, R.L. Powell, R.W. Lindsay, M. Yuan, A. Carpov, A. Wilson, M. Lopez, J.W. Coleman, D. Wagner, P. Sharma, M. Kemelman, K.J. Wright, J.P. Seabrook, H. Arendt, J. Martinez, J. DeStefano, M.J. Chiuchiolo, C.L. Parks, A novel, live-attenuated vesicular stomatitis virus vector displaying conformationally intact, functional HIV-1 envelope trimers that elicits potent cellular and humoral responses in mice, PLoS ONE 9 (9) (2014), e106597, https://doi.org/10.1371/journal.pone.0106597.

[4] S.E. Witko, C.S. Kotash, R.M. Nowak, J.E. Johnson, L.A. Boutilier, K.J. Melville, S. G. Heron, D.K. Clarke, A.S. Abramovitz, R.M. Hendry, M.S. Sidhu, S.A. Udem, C. L. Parks, An efficient helper-virus-free method for rescue of recombinant paramyxoviruses and rhadoviruses from a cell line suitable for vaccine development, J. Virol. Methods 135 (1) (2006) 91–101, https://doi.org/10.1016/j.jviromet.2006.02.006.